Novel Monte Carlo Molecular Simulation Scheme Using Identity-Altering Elementary Moves for the Calculation of Structure and Thermodynamic Properties of Polyolefin Blends

Loukas D. Peristeras,† Anastassia N. Rissanou,† Ioannis G. Economou,† and Doros N. Theodorou*,†,‡

Molecular Thermodynamics and Modelling of Materials Laboratory, Institute of Physical Chemistry, National Center for Scientific Research "Demokritos", GR-153 10 Aghia Paraskevi, Attikis, Greece, and Department of Materials Science and Engineering, School of Chemical Engineering, National Technical University of Athens, 9 Heroon Polytechniou Street, GR-157 80 Athens, Greece

Received November 25, 2006; Revised Manuscript Received February 4, 2007

ABSTRACT: In this work, the semi-grand statistical ensemble formalism proposed by Pant and Theodorou (*Macromolecules,* **1995,** *28,* 7224) for polydisperse melts of linear chains is extended to mixtures of linear and branched chains in order to calculate stability of binary polymer blends based on Monte Carlo simulation. Furthermore, a new elementary Monte Carlo move is introduced that consists of chain identity-altering between branched and linear chain species and thus allows fluctuations in the blend composition. The new move, together with previously developed moves for long chain molecules, are shown to relax efficiently both the branched and the linear molecules in binary linear polyethylene−triarm polyethylene blends of various macromolecular sizes. Subsequently, they are used for the calculation of the microscopic structure and the thermodynamic properties of these systems. All blends examined are shown to be fully miscible.

1. Introduction

Polymer blends have attracted considerable interest in recent years both in the research community and in industry.[1,2] The superior mechanical, electrical, thermophysical, optical, rheological, and other properties of many polymer blends and their favorable cost in comparison to their corresponding polymer components have encouraged the use of these materials in a wide range of industrial applications. In all these applications, a better understanding and an ability to predict blend properties from chemical constitution and composition is crucial. An important issue is the miscibility of the polymers in a blend. For most applications, it is desirable that the phase behavior of the polymer blend be accurately known, since it will affect its physical properties and, consequently, its processability and performance in the end-use environment. In parallel, the "molecular engineering" design of new polymeric materials based on blends with tailored properties is of great interest. This work focuses on polyolefin blends, a widely used and extensively studied but still incompletely understood class of polymer blends.

A large number of experimental groups worldwide has devoted considerable effort in studying the thermodynamics and phase behavior of blends of polymers that differ in macromolecular architecture, polarity, macromolecular size, and composition. A wide range of state-of-the art methods, including small-angle neutron scattering (SANS), small-angle X-ray scattering (SAXS), small-angle light scattering (SALS), solid-state NMR, and atomic force microscopy (AFM) were used for such purposes.[3−10] It is clear today that binary polyolefin blends exhibit all different types of fluid phase equilibria, such as upper critical solution temperature (UCST), lower critical solution temperature (LCST), and even both UCST and LCST at different temperatures.[11] Despite extensive work by different research groups, the phase behavior of many common polymer blends, as for example high-density polyethylene−low-density polyethylene (HDPE−LDPE), is not fully understood yet.[12−14] Such difficulty is rooted in experimental uncertainties, due to the similarity in the constituent groups of the polymers that does not allow clear contrast in scattering experiments. Partial deuteration of one of the polymers does not alleviate the problem fully.[10]

Molecular simulation is a reliable tool for the elucidation of microscopic mechanisms that control macroscopic behavior and subsequent calculation of thermodynamic properties and phase behavior. Molecular dynamics (MD) is a convenient method for the simulation of non-polymeric systems. However, for polymers that exhibit long characteristic times for relaxation that cannot be captured with MD, Monte Carlo (MC) simulation is the preferable method. In this case, smart "elementary" moves are needed, so that important configurations are sampled efficiently. In recent years, a number of elementary MC moves were proposed specifically for such purposes. Some of the most widely used moves for polymers include: reptation,[15] configurational bias (CB),[16−18] concerted rotation (CONROT),[19−20] flip,[21] end-bridging (EB),[20,22] and double-bridging (DB).[23] All of these moves were designed primarily for linear molecules and relax efficiently an internal or a terminal part of the chain molecule.

Recently, two new elementary moves were proposed for branched chain molecules:[24] Branch point flip (BPF) results in a displacement in space of a branch point and its neighboring atoms in the molecule without change in the connectivity. Wick and Siepmann have proposed a similar elementary move named self-adapting fixed-end-point configurational-bias for the simulation of small branched and cyclic alkanes.[25] An additional

* Author to whom all correspondence should be addressed. E-mail: doros@central.ntua.gr.

† Molecular Thermodynamics and Modelling of Materials Laboratory, Institute of Physical Chemistry, National Center for Scientific Research "Demokritos".

‡ Department of Materials Science and Engineering, School of Chemical Engineering, National Technical University of Athens.

10.1021/ma0627121 CCC: $37.00
Published on Web 03/16/2007

move proposed is the so-called branch point slithering (BPS) that allows for branch point displacement along the backbone;[24] in this case, the size of the branches involved is changed. In this work, we further extend these moves by introducing the identity-altering (IA) elementary move for systems consisting of linear and branched molecules. The IA move is an intermolecular bridging move where part of or an entire branch of a linear or a branched chain is cut and appended to a different chain (either linear or branched). In this way, the local configuration changes dramatically and, in addition, the mixture composition (linear vs branched) is altered. It is shown that the new move results in efficient relaxation of linear and branched chain molecules.

In a typical phase equilibrium calculation using MC simulation, molecules of the various components involved are moved from one phase to another.[26] In some cases, the chemical potential of one or more of the components needs to be evaluated.[27] Both operations become very cumbersome, if not impossible, for polymer systems. A number of alternative methodologies have been proposed to overcome such restrictions.[28−30] A useful approach is the use of a semi-grand statistical ensemble allowing interconversion between different components, wherein appropriate differences in chemical potential between the components are specified.

In this work, the new move is developed in the semi-grand statistical ensemble of Pant and Theodorou[20] extended to pseudobinary mixtures. The chemical potential difference between the two components is specified and the system composition is calculated. In this way, a single phase system is studied and no chemical potential calculation is needed. The proposed method is applied to mixtures of linear polyethylene and triarm polyethylene of the same molecular weight. Microscopic structure, chain sizes, and thermodynamic properties are reported. For all of the mixtures examined, the two components exhibit similar characteristics and so are fully miscible. A similar methodology has been proposed by Kofke and Glandt for simple Lennard-Jones binary mixtures.[31,32]

2. Development of the Statistical Ensemble

2.1. Definition of the System. The system under consideration consists of N polymer chains of which N_l are linear and N_b are branched, so that $N = N_l + N_b$. The total number of atoms is n. A branch (or an arm) is defined as the linear part of a chain that connects a chain end or a branch point with another chain end or branch point of the chain. Consequently, a linear chain is considered as a single branch and a branched chain consists of at least three branches. In general, every component k has b_k branch points. The number of atoms in each branch q is denoted by ν_q. Every branch point (bp) of the chain is characterized by the functionality index, f_{bp}, which is the number of branches attached to it. All branched chains in the system are assumed to have the same macromolecular architecture (they can be stars, H-shaped, brushes, etc.) with N_{br}^{ch} branches per chain. Therefore, $b_k = 0$ for linear chains and $b_k = b$ for branched chains, and

$$N_{br}^{ch} = 1 + (f_{bp} - 1)b \tag{1}$$

The branched chains that we will examine here are assumed to have $f_{bp} = 3$, so that $N_{br}^{ch} = 1 + 2b$.

2.2. The Statistical Ensemble. The statistical ensemble is a generalization of the semi-grand [$NnPT\boldsymbol{\mu}^*$] canonical ensemble of Pant and Theodorou[20] for a mixture of linear and branched polymers with branches of variable mean molecular weight. For this mixture, changes in the Helmholtz free energy (A) are given by the following expression:

$$\mathrm{d}A = -S\,\mathrm{d}T - P\,\mathrm{d}V + \sum_{k=1}^{m} \mu_k\,\mathrm{d}N_k \tag{2}$$

where S, T, P, and V are the entropy, temperature, pressure, and volume of the system, respectively, N_k and μ_k are the number of molecules and the chemical potential of component k, respectively, and m is the total number of components in the system.

The partition function of the canonical ensemble for the system is

$$Q(V,T,N_1,N_2,...,N_m) = \frac{1}{N_1!N_2!...N_m!}\frac{1}{\Lambda^{3n}}Z(V,T,N_1,N_2,...,N_m) \tag{3}$$

where $Z(V,T,N_1,N_2,..,N_m)$ is the configurational integral, equal to

$$Z(V,T,N_1,N_2,...,N_m) = \int \mathrm{d}^{3n}\mathbf{r}\,\exp[-\beta \boldsymbol{V}(\mathbf{r}_1,\mathbf{r}_2,...,\mathbf{r}_n)] \tag{4}$$

with $\mathbf{r}_i$ being the Cartesian coordinates of atom i, $\beta = 1/k_BT$ (k_B is the Boltzmann constant), Λ the monomer (atom) thermal wavelength, and $\boldsymbol{V}$ the potential energy function.

In the system under consideration, the total numbers of chains and of atoms are calculated from the expression

$$\sum_{k=1}^{m} N_k = N \tag{5}$$

$$\sum_{k=1}^{m} n_k N_k = n \tag{6}$$

with n_k being the number of atoms in a chain of species k.

Selecting an arbitrary pair of components i and j as reference components, variables N_i and N_j can be eliminated by invoking eqs 5 and 6 in favor of n and N. In this way, eq 2 results in

$$\mathrm{d}A = -S\,\mathrm{d}T - P\,\mathrm{d}V + \sum_{\substack{k=1 \\ k\neq i,j}}^{m} \mu_k^*\,\mathrm{d}N_k + \mu^{(n)}\,\mathrm{d}n + \mu^{(N)}\,\mathrm{d}N \tag{7}$$

where

$$\mu_k^* = \mu_k + \left(\frac{n_k - n_j}{n_j - n_i}\right)\mu_i - \left(\frac{n_k - n_i}{n_j - n_i}\right)\mu_j \tag{8}$$

$$\mu^{(n)} = \frac{\mu_i - \mu_j}{n_i - n_j} \tag{9}$$

$$\mu^{(N)} = \frac{n_i\mu_j - n_j\mu_i}{n_i - n_j} \tag{10}$$

A Legendre transformation of the Helmholtz free energy with respect to V and N_k, $k = 1, 2, ..., m$: $k \neq i, j$, results in the thermodynamic potential Y:

$$Y = A + PV - \sum_{\substack{k=1 \\ k\neq i,j}}^{m} \mu_k^* N_k \tag{11}$$

$$\mathrm{d}Y = -S\,\mathrm{d}T + V\,\mathrm{d}P - \sum_{\substack{k=1 \\ k\neq i,j}}^{m} N_k \mathrm{d}\mu_k^* + \mu^{(n)}\,\mathrm{d}n + \mu^{(N)}\,\mathrm{d}N \tag{12}$$

The partition function $\tilde{Y}$ of the statistical ensemble that corresponds to this potential is related to Y through the expression

$$Y = -k_B T \ln(\tilde{Y}) \tag{13}$$

and is equal to

$$\tilde{Y} = \sum_{\substack{\{N_1,N_2,\ldots,N_m\}: \\ \sum_{k=1}^{m} N_k = N}} \exp\left[\beta \sum_{\substack{k=1 \\ k\neq i,j}}^{m} \mu_k^* N_k\right] \frac{1}{V_0} \int_0^\infty \mathrm{d}V \times \exp[-\beta PV] Q(V,T,N_1,N_2,\ldots,N_m) \tag{14}$$

Consequently, the probability density function of this ensemble is

$$\rho^{NnPT\boldsymbol{\mu}^*}(V,\mathbf{r}_1,\mathbf{r}_2,\ldots,\mathbf{r}_n;\text{connectivity}) \propto \exp\left[\beta \sum_{\substack{k=1 \\ k\neq i,j}}^{m} \mu_k^* N_k - \beta PV - \beta \boldsymbol{V}(\mathbf{r}_1,\mathbf{r}_2,\ldots,\mathbf{r}_n;\text{connectivity})\right] \tag{15}$$

2.3. Size Distribution of the Chain Branches. Given the fact that that the number of branch points per branched chain remains constant, one may invoke the conformal solution principle for the configurational integral:[20]

$$Z(V,T,N_1,N_2,\ldots,N_m) = Z(V,T,N,n,N_b) \tag{16}$$

According to eq 16, the configurational integral depends on the number-averaged molecular weight, density of monomers and mole fraction of branched (or linear) chains but not on the details of the chain length distribution of linear and branched species. This assumption has been shown to be satisfactory for systems of sufficiently long linear polyethylene chains.[20] Equation 16 allows us to treat our system as a pseudobinary, consisting of linear and branched chains.

In the thermodynamic limit ($N_i \to \infty$, $i = 1, 2, \ldots, m$, all intensive properties of the system being kept constant) by invoking the maximum term approximation and using eqs 5, 6, and 16, eq 14 becomes

$$\tilde{Y} \propto \exp\left[\beta \sum_{\substack{k=1 \\ k\neq i,j}}^{m} \mu_k^* N_k - \beta PV - \sum_{k=1}^{m} N_k \ln N_k + \sum_{k=1}^{m} N_k - 3n\ln\Lambda + \ln Z(V,T,N,n,N_b)\right] \tag{17}$$

Maximization of $\tilde{Y}$ is equivalent with maximization of the term in brackets in eq 17 with the constraints that the total number of molecules N and the total number of monomers n remain constant. The method of Lagrange multipliers is used for this purpose. The expressions for the partial derivatives of the term under consideration, where ξ, ψ are the Lagrange multipliers that correspond to the constraints of eqs 5 and 6, respectively, are

$$\frac{\partial}{\partial N_s}[\text{term of eq 17 in brackets} + \xi(\sum_{k=1}^{m} N_k - N) + \psi(\sum_{k=1}^{m} n_k N_k - n)] = 0 \tag{18}$$

where $s = 1, 2, \ldots, m$. Equation 18 for the various species s becomes

$$\beta\mu_s^* - \ln(N_s) + \frac{\partial \ln(Z)}{\partial N_b}\frac{\partial N_b}{\partial N_s} + \xi + \psi n_s = \beta\mu_s^* - \ln(N_s) + \zeta\frac{b_s}{b} + \xi + \psi n_s = 0 \Rightarrow$$
$$N_s = c y^{n_s} z^{b_s/b} \exp[\beta\mu_s^*],\ s = 1,2,\ldots,m:\ s \neq i, j \tag{19}$$

$$-\ln(N_i) + \zeta\frac{b_i}{b} + \xi + \psi n_i = 0 \Rightarrow N_i = c y^{n_i} z^{b_i/b} \tag{20}$$

$$-\ln(N_j) + \zeta\frac{b_j}{b} + \xi + \psi n_j = 0 \Rightarrow N_j = c y^{n_j} z^{b_j/b} \tag{21}$$

where $c = \exp[\xi]$, $y = \exp[\psi]$, $z = \exp[\zeta]$, and $\zeta = (\partial\ln(Z))/(\partial N_b)$. Coefficients c and y can be calculated from eqs 5 and 6 for given z and μ_s^*.

Manipulating the composition of the system is possible by using different chemical potential values for each species. One of the possible sets of values for the statistical ensemble under consideration is

$$\mu_k^* = \begin{cases} 0 & \text{for } b_k = 0 \quad \text{[linear species with a given range of sizes]} \\ \mu^* & \text{for } b_k = b \quad \text{[branched species with a given range of branch sizes]} \\ -\infty & \text{all other cases} \end{cases} \tag{22}$$

which imposes the same chemical potential for all linear components, and the same relative chemical potential with respect to linear components for all branched components. Such an approach is meaningful for the case where all branched species have the same macromolecular architecture.

In eq 22, we have to specify the ranges of sizes for which the chemical potential differs from negative infinity and are therefore allowed in the system. Our intention is to impose a uniform distribution on the size of branches of the species present in the mixture, within a preselected range of values. This range is defined according to the expression:

$$\nu_q \in \begin{cases} [\bar{\nu}_l(1-\Delta_l),\ \bar{\nu}_l(1+\Delta_l)] & \text{for } b_q = 0 \\ [\bar{\nu}_q(1-\Delta_q),\ \bar{\nu}_q(1+\Delta_q)] & \text{for } b_q = b,\ q = 1, 2, \ldots, (1+2b) \end{cases} \tag{23}$$

where $\bar{\nu}_l$ is the mean chain size for linear chains and $\bar{\nu}_q$ is the mean branch size for branch q of a branched chain. Taking into account that the total number of segments in a branched chain is $b + \sum_{q=1}^{1+2b} \nu_q$, one obtains

$$N = c\sum_{\nu_k=\bar{\nu}_l(1-\Delta_l)}^{\bar{\nu}_l(1+\Delta_l)} y^{\nu_k} + czy^b \exp[\beta\mu^*] \prod_{q=1}^{1+2b} \sum_{\nu_q=\bar{\nu}_q(1-\Delta_q)}^{\bar{\nu}_q(1+\Delta_q)} y^{\nu_q} \quad (24)$$

$$n = c\sum_{\nu_k=\bar{\nu}_l(1-\Delta_l)}^{\bar{\nu}_l(1+\Delta_l)} \nu_k y^{\nu_k} + czy^b \exp[\beta\mu^*] \times \{b\prod_{q=1}^{1+2b}(\sum_{\nu_q=\bar{\nu}_q(1-\Delta_q)}^{\bar{\nu}_q(1+\Delta_q)} y^{\nu_q}) + \sum_{q=1}^{1+2b}(\sum_{\nu_q=\bar{\nu}_q(1-\Delta_q)}^{\bar{\nu}_q(1+\Delta_q)} \nu_q y^{\nu_q}) \times \prod_{\substack{q'=1\\q'\neq q}}^{1+2b}(\sum_{\nu_{q'}=\bar{\nu}_q(1-\Delta_q)}^{\bar{\nu}_q(1+\Delta_q)} y^{\nu_{q'}})\} \quad (25)$$

Given the fact that $y \rightarrow 1 \Rightarrow \psi \rightarrow 0$, this is equivalent with relaxing the constraint of the total number of monomer units being constant, which is possible if the branch size distribution is well-defined. In this way one may define the mean chain size and, since the total number of chains in the system is constant, then the total number of atoms will also be constant. For this reason, eqs 24 and 25 should have a solution for $y \rightarrow 1$ and so

$$N = c\sum_{\nu_k=\bar{\nu}_l(1-\Delta_l)}^{\bar{\nu}_l(1+\Delta_l)} [1] + cz[1]^b \exp[\beta\mu^*] \prod_{q=1}^{1+2b} \sum_{\nu_q=\bar{\nu}_q(1-\Delta_q)}^{\bar{\nu}_q(1+\Delta_q)} [1] = c(2\bar{\nu}_l\Delta_l + 1) + c\,z\exp[\beta\mu^*]\prod_{q=1}^{1+2b}(2\bar{\nu}_q\Delta_q + 1) \quad (26)$$

$$n = c\sum_{\nu_k=\bar{\nu}_l(1-\Delta_l)}^{\bar{\nu}_l(1+\Delta_l)} \nu_k + cz[1]\exp[\beta\mu^*]\{b\prod_{q=1}^{1+2b}\sum_{\nu_q=\bar{\nu}_q(1-\Delta_q)}^{\bar{\nu}_q(1+\Delta_q)}[1] + \sum_{q=1}^{1+2b}\bar{\nu}_q\prod_{q=1}^{1+2b}\sum_{\nu_q=\bar{\nu}_q(1-\Delta_q)}^{\bar{\nu}_q(1+\Delta_q)}[1]\}$$

$$= c\bar{\nu}_l(2\bar{\nu}_l\Delta_l + 1) + cz\exp[\beta\mu^*](b + \sum_{q=1}^{1+2b}\bar{\nu}_q) \times \prod_{q=1}^{1+2b}(2\bar{\nu}_q\Delta_q + 1) \quad (27)$$

If the mean size of linear chains ($\bar{X}_l$) is set equal to the mean size of branched chains ($\bar{X}_b$), then:

$$\bar{X} = \bar{X}_l = \bar{X}_b = \frac{n}{N};\quad \bar{X}_l = \bar{\nu}_l;\quad \bar{X}_b = b + \sum_{q=1}^{1+2b}\bar{\nu}_q \quad (28)$$

and the two equations become linearly dependent. In this way, eq 26 is solved for c:

$$c = \frac{N}{(2\bar{\nu}_l\Delta_l + 1) + z\exp[\beta\mu^*]\prod_{q=1}^{1+2b}(2\bar{\nu}_q\Delta_q + 1)} \quad (29)$$

2.4. Calculation of Mole Fractions. The c value calculated from eq 29 can be used for the evaluation of the number of molecules and consequently for the mole fraction of linear and branched species in the system under consideration:

$$N_l = c(2\bar{\nu}_l\Delta_l + 1) \quad (30)$$

$$N_b = cz\exp[\beta\mu^*]\prod_{q=1}^{1+2b}(2\bar{\nu}_q\Delta_q + 1) \quad (31)$$

and the mole fractions of linear and branched species become

$$x_l = \frac{2\bar{\nu}_l\Delta_l + 1}{2\bar{\nu}_l\Delta_l + 1 + z\exp[\beta\mu^*]\prod_{q=1}^{1+2b}(2\bar{\nu}_q\Delta_q + 1)} \quad (32)$$

$$x_b = \frac{z\exp[\beta\mu^*]\prod_{q=1}^{1+2b}(2\bar{\nu}_q\Delta_q + 1)}{2\bar{\nu}_l\Delta_l + 1 + z\exp[\beta\mu^*]\prod_{q=1}^{1+2b}(2\bar{\nu}_q\Delta_q + 1)} \quad (33)$$

2.5. Molecular Simulation Strategy. In our semi-grand canonical simulations we specify a profile of relative chemical potentials according to eqs 22 and 23. At equilibrium, the system responds with a certain composition (distribution of molecular species present). If the conformal solution assumption, eq 16, holds, then the size distributions of linear species and of branches belonging to branched species should be uniform within the ranges defined by eq 23. (This will be tested). Also, the equilibrium composition should conform to eqs 32 and 33. Having set μ^* and having obtained x_b as an output from molecular simulation, we may calculate z, which is a measure of the nonideality of mixing, through eq 32 or eq 33:

$$\text{eq } 33 \Rightarrow z = \frac{x_b}{1-x_b}\frac{2\bar{\nu}_l\Delta_l + 1}{\exp[\beta\mu^*]\prod_{q=1}^{1+2b}(2\bar{\nu}_q\Delta_q + 1)}$$

or

$$\beta\mu^* = \ln\left[\frac{2\bar{\nu}_l\Delta_l + 1}{z\prod_{q=1}^{1+2b}(2\bar{\nu}_q\Delta_q + 1)}\right] + \ln\left[\frac{x_b}{1-x_b}\right] \quad (34)$$

If the mixture is ideal, then (compare also eq 41 below):

$$\zeta = \frac{\partial\ln(Z)}{\partial N_b}\bigg|_{V,T,N,n} = \text{constant} \Rightarrow z = \exp[\text{constant}] \quad (35)$$

and so z is independent of the composition. For this value of z, the composition dependence of $\beta\mu^*$ is identical to the dependence for an ideal solution:

$$\beta\mu^{*,id} = \beta(\mu_b - \mu_l) = \beta(\mu_{b,pure} - \mu_{l,pure}) + \ln\left[\frac{x_b}{1-x_b}\right] \quad (36)$$

Molecular simulation provides the dependence of μ^* on the mole fraction of branched species, $\mu^*(x_b)$. From this dependence, the activity coefficients of the components can be evaluated. For the binary linear chain−branched chain mixture under consideration, the Gibbs−Duhem equation under constant temperature and pressure results in

$$\left.\begin{aligned}(1-x_b)\,d\mu_l|_{T,P} + x_b\,d\mu_b|_{T,P} = 0\\ d\mu_l|_{T,P} - d\mu_b|_{T,P} = d\mu^*|_{T,P}\end{aligned}\right\} \Rightarrow \left\{\begin{aligned}d\mu_b|_{T,P} = (1-x_b)\,d\mu^*|_{T,P}\\ d\mu_l|_{T,P} = -x_b\,d\mu^*|_{T,P}\end{aligned}\right\} \quad (37)$$

Taking the reference state for each component as the pure component at the mixture temperature and pressure, we can write for the activity coefficients γ_b, γ_l of the branched and linear species, respectively:

$$\left.\begin{aligned}\mu_b &= \mu_{b,pure} + k_B T \ln(\gamma_b x_b)\\ \mu_l &= \mu_{l,pure} + k_B T \ln(\gamma_l x_l)\end{aligned}\right\} \Rightarrow$$
$$\left.\begin{aligned}\beta\, d\mu_b|_{T,P} &= \frac{dx_b}{x_b} + d(\ln(\gamma_b))\\ \beta\, d\mu_l|_{T,P} &= -\frac{dx_b}{1-x_b} + d(\ln(\gamma_l))\end{aligned}\right\} \Rightarrow$$
$$\left.\begin{aligned} d(\ln(\gamma_b))|_{T,P} &= (1-x_b)\beta\, d\mu^*|_{T,P} - \frac{dx_b}{x_b}\\ d(\ln(\gamma_l))|_{T,P} &= -x_b\beta\, d\mu^*|_{T,P} + \frac{dx_b}{1-x_b}\end{aligned}\right\} \Rightarrow$$
$$\left.\begin{aligned}\frac{d\ln(\gamma_b)}{dx_b}\bigg|_{T,P} &= (1-x_b)\beta\frac{d\mu^*}{dx_b}\bigg|_{T,P} - \frac{1}{x_b}\\ \frac{d\ln(\gamma_l)}{dx_b}\bigg|_{T,P} &= -x_b\beta\frac{d\mu^*}{dx_b}\bigg|_{T,P} + \frac{1}{1-x_b}\end{aligned}\right\} \Rightarrow$$
$$\left.\begin{aligned}\ln(\gamma_b) &= \int_{x_b}^{1}\left[\frac{1}{x_b} - (1-x_b)\beta\frac{d\mu^*}{dx_b}\bigg|_{T,P}\right]dx_b\\ \ln(\gamma_l) &= \int_{0}^{x_b}\left[\frac{1}{1-x_b} - x_b\beta\frac{d\mu^*}{dx_b}\bigg|_{T,P}\right]dx_b\end{aligned}\right\} \quad (38)$$

The thermodynamic eqs 37, 38 are perfectly general for a two-component system.

According to the definition of z:

$$z = \exp[\zeta] = \exp\left[\frac{\partial(\ln(Z))}{\partial N_b}\bigg|_{V,T,N,n}\right] \quad (39)$$

and the standard thermodynamic expression:

$$\mu^* = \mu_b - \mu_l = \mu_{b,pure} - \mu_{l,pure} + \frac{1}{\beta}\ln\left(\frac{\gamma_b}{\gamma_l}\right) + \frac{1}{\beta}\ln\left[\frac{x_b}{1-x_b}\right] \quad (40)$$

z can be expressed as a function of the activity coefficients:

$$z = \frac{\gamma_l}{\gamma_b}\exp[-\beta(\mu_{b,pure}(T,P) - \mu_{l,pure}(T,P))]\exp[\beta(\mu^{ig}_{b,pure}(T,P^{ig}) - \mu^{ig}_{l,pure}(T,P^{ig}))]\frac{Z_b^{intra}}{Z_l^{intra}} \quad (41)$$

where $P^{ig} = \rho k_B T$, ρ is the total molecular density of the system and Z_i^{intra} is the intramolecular configurational integral over all orientations and over all conformations of species i in the ideal gas state. Equation 41 indicates that z depends on the ratio of activity coefficient values.

Finally, the system stability can be assessed; for a stable single-phase mixture, we must have[33]

$$x_b\frac{d(\ln(\gamma_b))}{dx_b}\bigg|_{T,P} + 1 \geq 0 \Rightarrow \frac{d\mu^*}{dx_b}\bigg|_{T,P} \geq 0 \quad (42)$$

In Figure 1, a schematic representation of the variation of μ^* as a function of composition, x_b, is shown for a fully miscible and a partially miscible mixture.

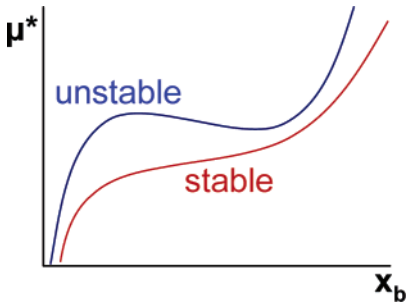

Figure 1. Schematic representation of the dependence of the relative chemical potential of branched chains, μ^*, as a function of the composition, x_b, for a binary mixture of linear and branched chains. For a stable mixture μ^* varies monotonically with the composition, whereas for an unstable mixture μ^* goes through a local maximum and a local minimum value (points on the spinodal) that define the region of instability of the one-phase mixture.

3. Identity-Altering Elementary Monte Carlo Moves

The systems examined in this work are binary mixtures of linear chains and branched chains with a single trifunctional branch point (triarm chains), so that $f_{bp} = 3$ and $b = 1$. In a recent work,[24] a number of elementary MC moves were proposed specifically for long-chain branched molecules. Here, we further extend this approach by developing moves that allow IA, that is conversion from a linear chain to a branched chain and vice versa. As in previous publications,[20,24] the derivation is formulated in the $(N,n,P,T,\boldsymbol{\mu}^*)$ semi-grand statistical ensemble. These moves allow efficient convergence of the mole fraction to the value that corresponds to the equilibrium under the set thermodynamic conditions (chemical potential difference, temperature, pressure). The new moves combine previously developed moves for chain molecules, such as CB and EB, so that a branch, or part of it, is transferred from one chain to another chain. In Figure 2, the four different ways by which the identity of chains is altered according to the moves developed here are shown. Every branch that is involved in a move may contain additional smaller branches, so that this set of moves can be further extended to more complex systems. The details of these moves are presented below.

3.1. Branch Creation (BC) Move. A branch is created through a chain cut and connection to a linear chain. This move (BC, in short) is shown schematically in Figure 3. In all cases, a trimer is relocated in the spirit of the CONROT move.[19−20] The BC move is implemented in two steps:

(a) Initially, the end-bridging move is used so that the branch is connected to its new position. One of the terminal four atoms (a, b, c, d) of the "donor" chain "attacks" atom iv that was selected from a list of candidates (fulfilling the MW distribution constraints) as the new branch point on the "acceptor" chain. For the connection of the new branch, the following strategy is used: The "donor" chain is cut at a randomly selected point (in Figure 3, it is cut between atoms 5 and 6). The atoms necessary to form the first atom of the new branch and to bridge it with the branch point are taken from the vicinity of the cut point. For example, if atom b "attacks" atom iv, then atoms 6 and 7, along with atom a, should be used to construct a trimer bridge between atom iv and atom b.

(b) In order to relax the nonbonded interactions in the vicinity of the cut point, a number of atoms are repositioned using the CB algorithm. For example, with reference to Figure 3, if atom c "attacks" atom iv, then atom 6 is cut and moved to assist the

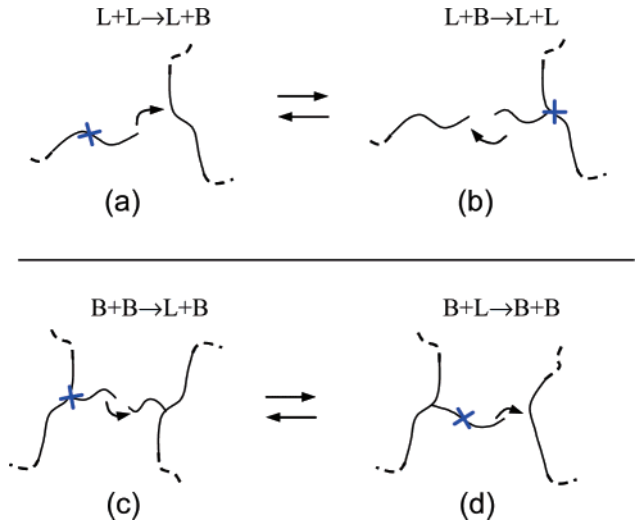

Figure 2. Schematic representation of IA elementary moves using intermolecular rebridging: In (a), a linear chain "attacks" another linear chain in order to form a branch. In the reverse move (b), a linear chain "attacks" a branched chain in order to incorporate one of its branches. In (c), a branched chain "attacks" another branched chain in order to incorporate one of its branches, converting it to a linear chain. In the reverse move (d), a branched chain "attacks" a linear chain, providing to it part of one of its branches and converting it to a branched chain. In all cases, the cross defines the point where a branch is cut. In the accompanying "chemical equations", the moves are represented as bimolecular reactions.

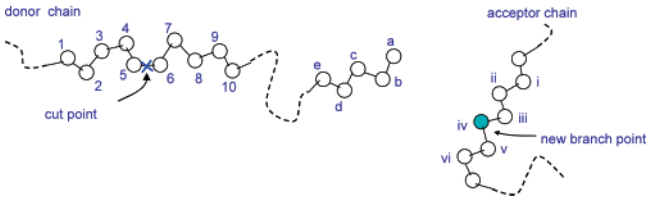

Figure 3. Schematic representation of the branch creation (BC) move. The donor chain may be a linear or a branched chain. Here, the donor chain is cut between atoms 5 and 6 and the new branch point in the acceptor chain is atom iv.

Table 1. Attack Atoms, Moving Atoms, and Repositioned Atoms for the BC Move (With Reference to Figure 3)[a]

		options for the atom repositioning			
attack atom	moving atoms	1st	2nd	3rd	4th
a	**6**, 7, **8**	none	none	none	none
b	**6**, **7**	5	**8**		
c	**6**	4, 5	5, 7	**7**, **8**	
d	none	3, 4, 5	4, 5, **6**	5, **6**, **7**	**6**, **7**, **8**

[a] The repositioned atoms in bold belong to the newly formed branch.

new branch bridging to the "acceptor" chain, while two atoms in the vicinity of the cut are repositioned. In Table 1, the various options concerning the attack atoms, the moving atoms and the repositioned atoms are shown.

3.2. Branch Destruction (BD) Move. Cutting a branch of a branched chain and connecting it with the end of another chain results in the creation of a linear chain. This move (BD, in short) is in essence the opposite of the BC move (three atoms are repositioned again) and takes place in two steps that are briefly presented here (see Figure 4):

(a) An end-bridging move is used initially in order to connect one of the four terminal atoms of the "donor" branch with a randomly selected atom from the "acceptor" chain (the latter atom should be located close to the acceptor chain end). Consequently, a number of atoms of the "donor" branch are relocated from the vicinity of the branch point to the bridging area.

(b) A number of atoms are repositioned in the vicinity of the branch point of the "donor" chain using the CB algorithm. In this case, this is necessary since the nonbonded interactions near the branch point are unrealistically high because of the increased local density.

3.3. Acceptance Criteria. The elementary moves presented above proceed as follows: A chain is randomly selected, followed by the random selection of one of its atoms close to a branch end (one of the four terminal atoms of a branch). This will be the "attack" atom. Furthermore, it is decided randomly whether the move will be the creation or destruction of either a linear or a branched chain. Finally, a tentative "acceptor" chain is selected.

The following microscopic reversibility equation is the starting point for the derivation of the acceptance criterion of a MC move:

$$a_{(o\to n)}\, A_{(o\to n)}\, P_{(o)} = a_{(n\to o)}\, A_{(n\to o)}\, P_{(n)} \tag{43}$$

where $a_{(i\to j)}$ is the conditional attempt probability of going from state i to state j, $A_{(i\to j)}$ is the conditional acceptance probability of going from state i to state j and $P_{(i)}$ is the equilibrium probability of the system being in state i. Subscripts o and n denote old and new states, respectively.

In a recent work on the development of elementary MC moves for the branch point of chain molecules,[24] the detailed derivation of acceptance probability for the branch point flip (BPF) and branch point slithering (BPS) moves were presented. The derivation of acceptance probability for BC or BD is based to a large extent on the same principles. In the bridge step and the atom reposition step of the BC move statistical weights, w_{bridge} and w_{cb} (cb here stands for configurational bias), respectively, are introduced. Consequently, the conditional attempt probability for the system to move from state i to state j is

$$a_{(i\to j)} = \frac{1}{N}\frac{1}{n_{\text{ep}}^{\text{ch}}}\frac{1}{2}\frac{1}{n_\nu}\, w_{\text{bridge}(i\to j)} w_{\text{cb}(i\to j)} \tag{44}$$

where N is the number of chains, $n_{\text{ep}}^{\text{ch}}$ is 2 for a linear chain and 3 for a branched chain, and n_ν is the number of terminal atoms in the chain that are possibly involved in the move (here $n_\nu = 4$). Finally, $a_{(i\to j)}$ accounts for the random selection of the type of chain (linear or branched) through the 1/2 term. Incorporation of eq 44 into the general expression for the acceptance criterion[24]

$$A_{(o\to n)} = \min\left(1, \frac{\prod_{s=1}^{\text{no. of steps}} a_{(n\to o),s}\rho_n \prod_{s=1}^{\text{no. of steps}} J_{n,s}}{\prod_{s=1}^{\text{no. of steps}} a_{(o\to n),s}\rho_o \prod_{s=1}^{\text{no. of steps}} J_{o,s}}\right) \tag{45}$$

results in the acceptance criterion for the branched chain creation move:

$$A_{(o\to n)} = \min\left(1, \frac{n_{\nu,o}\, w_{\text{bridge}(n\to o)}\, w_{\text{cb}(n\to o)} \exp(-\beta\mu^* - \beta \boldsymbol{V}_n) J_{\text{br,n}} J_{\text{cb,n}}}{n_{\nu,n}\, w_{\text{bridge}(o\to n)} w_{\text{cb}(o\to n)} \exp(-\beta \boldsymbol{V}_o) J_{\text{br,o}}}\right) \tag{46}$$

and the acceptance criterion for linear chain creation move:

$$A_{(o\rightarrow n)} = \min\left(1, \frac{w_{\text{bridge}(n\rightarrow o)}\, w_{\text{cb}(n\rightarrow o)} \exp(-\beta \boldsymbol{V}_n) J_{\text{br,n}}}{w_{\text{bridge}(o\rightarrow n)}\, w_{\text{cb}(o\rightarrow n)} \exp(-\beta\mu^* - \beta \boldsymbol{V}_o) J_{\text{br,o}} J_{\text{cb,o}}}\right) \quad (47)$$

The two Jacobians J_{br} and J_{cb} can be found in refs 34 and 16−18, respectively, and are not repeated here.

4. Simulation Details

In order to assess the proper implementation of the statistical ensemble, the correctness of the new elementary moves introduced and the overall efficiency of the method, ideal mixtures of phantom triarm symmetric polyethylene chains with their linear analogs were examined. In phantom chains only bond angle bending interactions are nonzero, whereas dihedral angle torsional potentials and all nonbonded intramolecular and intermolecular interactions are set equal to zero. Bond lengths were fixed in all calculations. Subsequently, the same mixtures were examined using full intra- and intermolecular interactions. The mean number of carbon atoms per chain ($\bar{X}$) was 61 ($\bar{\nu}_q =$ 20 carbon atoms per branch and a branch point), 121 ($\bar{\nu}_q = 40$ carbon atoms per branch and a branch point), or 301 ($\bar{\nu}_q = 100$ carbon atoms per branch and a branch point). The branch molecular weight distribution for the triarm chains and the chain molecular weight distribution for the linear chains were uniform in the interval $[\bar{X}(1-\Delta), \bar{X}(1+\Delta)]$ with $\Delta_l = \Delta_b = \Delta = 0.5$.

The simulation box contained a total number of 80 chains for the C_{61} mixture, 40 chains for the C_{121} mixture and 12 chains for the C_{301} mixture. In all cases, the temperature was set equal to 450 K and the pressure at 0.1 MPa. The relative chemical potential values, μ^*, were varied between $-10k_BT$ and $0k_BT$ for the phantom chain mixtures and between $-4k_BT$ and $5k_BT$ for the real mixtures. A typical MC simulation run, unless otherwise indicated, consisted of the following elementary moves: 10% reptation, 4% end-rotation, 19% CONROT, 25.5% EB, 0.5% volume fluctuation, 3% DF, 4% BPF, 4% BPS, and 30% chain IA. All simulations were performed on AMD Athlon MP 1800+ processors. A typical run consisted of 5×10^7 MC moves. The acceptance rate for the chain IA move was on the order of 0.02% which is a typical value for such complex elementary moves that result in drastic changes of the configuration.

In all cases the force field employed was TraPPE-UA, an accurate united atom (UA) force field developed for thermodynamic properties of linear and branched alkanes and later extended to other classes of organic compounds.[35,36] In TraPPE bond lengths are kept constant, whereas bond angle bending and dihedral angle torsions are calculated using appropriate expressions. Finally, nonbonded intra- and intermolecular interactions are calculated from the Lennard-Jones potential with parameters fitted to saturated liquid density and vapor pressure experimental data.

5. Results and Discussion

5.1. Mixtures of Phantom Chains. In order to assess the proper implementation of the new statistical ensemble with the new chain IA MC move, ideal mixtures of phantom triarm and phantom linear chains of the same mean molecular weight were examined. For a given relative chemical potential value, the run consisted of 5×10^6 MC moves and the CPU time was 2.6×10^4 s. The moves used were 10% reptation, 4% end-rotation, 10% flip, 10% CONROT, 24.5% EB, 0.5% volume fluctuation, 3% DF, 4% BPF, 4% BPS, and 30% chain IA.

In Figure 5, the normalized distribution of the two types of bond angles for the C_{121} triarm chains is shown. For comparison, the theoretical distribution ($\propto \sin(\theta) \exp[-\beta U_{\text{bend}}(\theta)]$) calculated from the TraPPE-UA force field is plotted. The two sets of calculations (molecular simulation and model predictions) coincide over the entire spectrum of bond angle values. Furthermore, the normalized distribution of torsion angles for these chains is shown in Figure 6, together with the theoretically expected uniform distribution. In a phantom chain, all torsion angle values are equally probable. Indeed, the moves used do not impose any bias in the torsion angle distribution; this

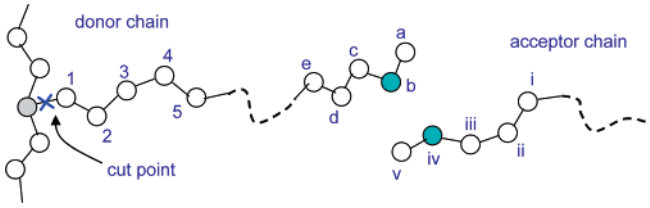

Figure 4. Schematic representation of the branch destruction (BD) move. The acceptor branch may be part of a linear or a branched chain. Here, the branch is cut at the cross and bridging occurs between atoms b and iv of the two different branches.

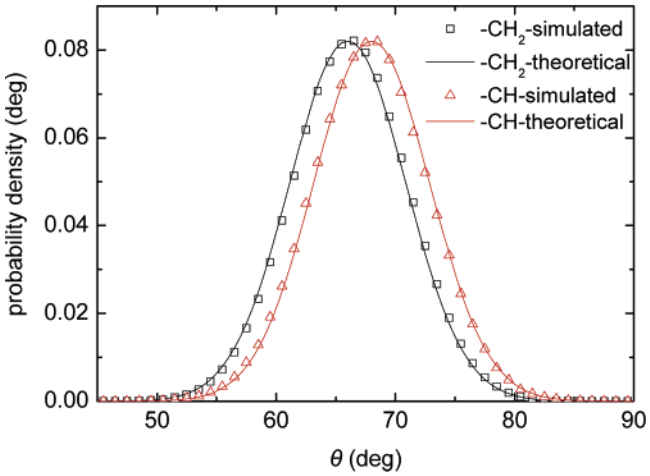

Figure 5. Normalized distribution of the bond angles centered at the $-CH_2-$ and the $-CH-$ UA, respectively, of phantom C_{121} triarm ($3 \times 40 + 1$) chains in a mixture with their linear analogs at 450 K, 0.1 MPa and $\beta\mu^* = -5$. The solid lines display the theoretical distributions based on the TraPPE-UA force field, and the points are simulation results.

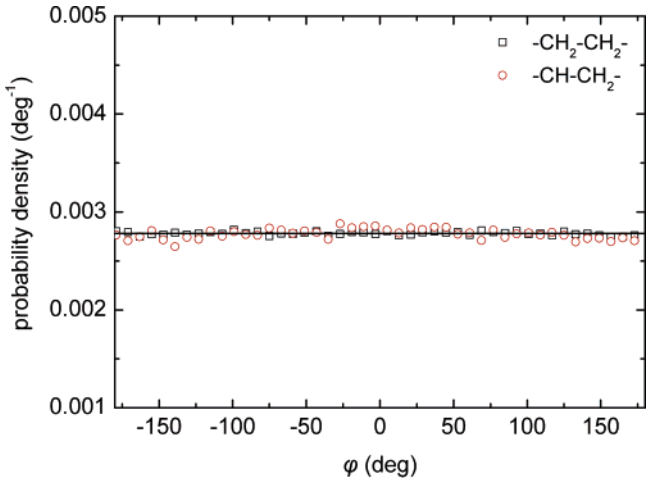

Figure 6. Normalized distribution of the torsion angles around the $-CH_2-CH_2-$ and the $-CH-CH_2-$ bonds, respectively, of phantom C_{121} triarm ($3 \times 40 + 1$) chains in a mixture with their linear analogs at 450 K, 0.1 MPa and $\beta\mu^* = -5$. There is no torsional potential and so a uniform distribution is expected (solid line), which also results from simulation.

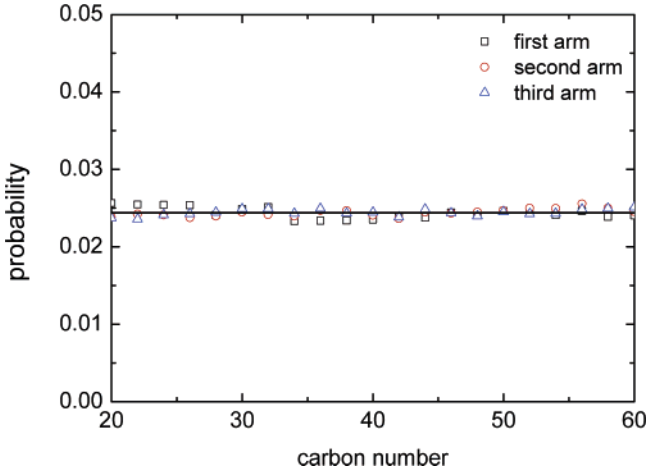

Figure 7. Probability distribution of the length (in carbon atoms) of each of the three arms of phantom C_{121} triarm ($3 \times 40 + 1$) chains in a mixture with their linear analogs at 450 K, 0.1 MPa and $\beta\mu^* = -5$.

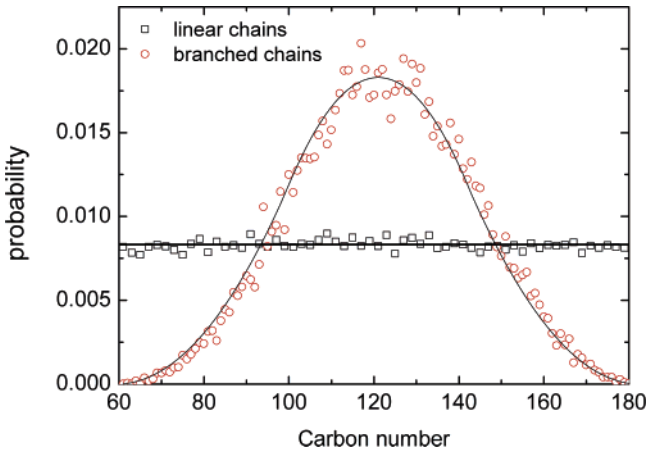

Figure 8. Probability distribution of the molecular size (in carbon atoms) of phantom C_{121} triarm ($3 \times 40 + 1$) chains and of linear C_{121} linear chains in a mixture at 450 K, 0.1 MPa and $\beta\mu^* = -5$. The solid curve is the exact mathematical expression for this distribution.[24]

provides a strong indication that the moves have been implemented properly.

In Figure 7, the ability of the elementary moves used to provide uniform sampling of all arm lengths allowed, based on the chemical potential values imposed (eq 22), is shown. The mean carbon number per arm is 40 and $\Delta = 0.5$, so that the allowable arm size is between 20 and 60 carbon atoms. A uniform distribution (within a statistical uncertainty) is obtained, ensuring the proper implementation of the move.

The probability distribution of the size of the entire phantom triarm chain is calculated based on the distribution of the individual arms (Figure 8). The shape of this distribution is close to a Gaussian and the exact mathematical expression for it was presented in eq 21 of ref 24. Simulation results follow very closely the theoretical curve. In Figure 8, the probability distribution for the size of linear chains of the same mixture is shown. A uniform distribution is obtained within the predefined range of sizes, thus ensuring a proper implementation of the method.

The statistical ensemble examined in this work allows accurate estimation of the mixture composition for a given relative chemical potential value. Consequently, MC simulation of binary mixtures at various chemical potential values can used to evaluate the entire x_b vs μ^* curve and thus estimate the mixture stability. In Figure 9, simulation results for three ideal

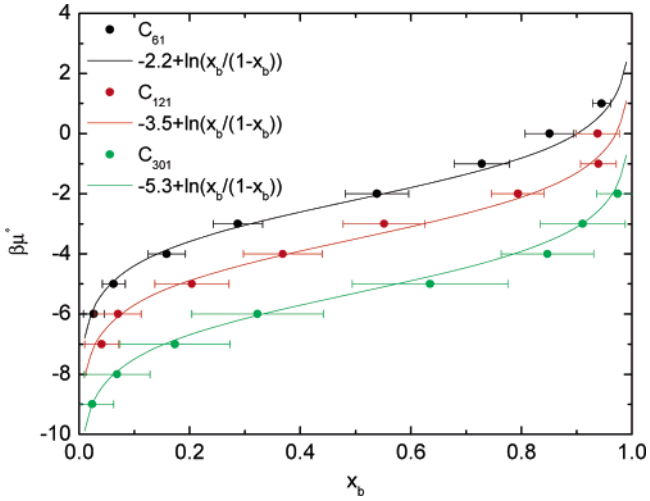

Figure 9. Relative chemical potential, $\beta\mu^*$, as a function of composition, x_b, for the mixtures: (a) phantom linear C_{61}−phantom triarm C_{61} ($3 \times C_{20} + 1$), (b) phantom linear C_{121}−phantom triarm C_{121} ($3 \times C_{40} + 1$), and (c) phantom linear C_{301}−phantom triarm C_{301} ($3 \times C_{100} + 1$). Points are simulation results, and lines are best fits to the data assuming a composition independent z.

phantom linear chain−triarm chain mixtures differing in the size of the chains are shown. The mean carbon number of linear and triarm chains in the first mixture is 61, in the second mixture it is 121, while in the third mixture it is 301. In all cases, mixtures exhibit a monotonic dependence of μ^* on x_b and thus the mixtures are fully stable, as expected of course. For such ideal mixtures, z is composition independent (eq 35) and thus the first term in eq 34 assumes a constant value based on the mixture chain characteristics (mean arm size, arm size distribution, and linear chain size distribution). Indeed, in Figure 9, the calculated $\beta\mu^*$ curves are shown for the three mixtures, assuming that z is composition independent (compare eq 41). The coefficients shown in the legend result from best fits to the simulation data. Note that simulation results for all pairs (i.e., C_{61}−C_{121}, C_{61}−C_{301} and C_{121}−C_{301}) of mixtures differ by a constant value for all compositions. These offsets are calculable from eq 34, if one assumes that z is the same in all three ideal gas phantom chain mixtures:

$$\beta\mu^*_{C_{121}} - \beta\mu^*_{C_{61}} = \ln\left[\frac{2 \times 120 \times 0.5 + 1}{(2 \times 40 \times 0.5 + 1)^3}\right] - \ln\left[\frac{2 \times 60 \times 0.5 + 1}{(2 \times 20 \times 0.5 + 1)^3}\right] = -1.3 \quad (48a)$$

$$\beta\mu^*_{C_{301}} - \beta\mu^*_{C_{61}} = \ln\left[\frac{2 \times 300 \times 0.5 + 1}{(2 \times 100 \times 0.5 + 1)^3}\right] - \ln\left[\frac{2 \times 60 \times 0.5 + 1}{(2 \times 20 \times 0.5 + 1)^3}\right] = -3.1 \quad (48b)$$

$$\beta\mu^*_{C_{301}} - \beta\mu^*_{C_{121}} = \ln\left[\frac{2 \times 300 \times 0.5 + 1}{(2 \times 100 \times 0.5 + 1)^3}\right] - \ln\left[\frac{2 \times 120 \times 0.5 + 1}{(2 \times 40 \times 0.5 + 1)^3}\right] = -1.8 \quad (48c)$$

On the other hand, the offsets between $\beta\mu^*(x_b)$ curves can be calculated analytically for such phantom chain ideal gas mixtures. Using Mathematica, the following values were obtained:

$$\beta\mu^*_{C_{121}} - \beta\mu^*_{C_{61}} = -1.2, \quad \beta\mu^*_{C_{301}} - \beta\mu^*_{C_{61}} = -2.9,$$
$$\beta\mu^*_{C_{301}} - \beta\mu^*_{C_{121}} = -1.7$$

which are in very good agreement (within statistical error) with both the estimates of eq 48 above and with the best fits to the simulation results, given in the legend to Figure 9.

5.2. Real Polyolefin Blends. The three binary blends were further studied in the semi-grand statistical ensemble introduced here using TraPPE-UA, a fully realistic intra- and intermolecular potential.[35,36] Initially, the molecular size characteristics of the two components were examined to ensure proper implementation of the method. For the C_{61} mixture, the probability distribution of the arm length for the triarm molecules and the probability distribution of the overall chain size for the linear and triarm molecules, both measured in carbon atoms, are shown in Figures 10 and 11, respectively. Both distributions follow the theoretically expected curves based on the conformal solution assumption. Furthermore, the molecular size distribution of the triarm polyethylene is considerably less noisy than the size distribution of the same species in the C_{121} ideal mixture (Figure 7 for the arms and Figure 8 for the chain). This should be attributed to the larger number of chains in the C_{61} mixture (80 chains) compared to the C_{121} mixture (40 chains) and to the longer run times.

The spatial extent of the molecules was examined for the mixtures of linear and triarm polyethylene. For the root-mean-square radius of gyration of polymer chains, the following scaling equation holds[37]

$$\langle R_g^2 \rangle^{1/2} \sim X^{\upsilon} \tag{49}$$

where X is the number of carbon atoms in the polymer and υ is 0.5 for the case of unperturbed chains and 0.6 for the case of good solvent conditions. In general, polymer melts exhibit unperturbed chain behavior. In Figure 12, a double logarithmic plot of $\langle R_g^2 \rangle$ vs carbon number is shown for the two components in the C_{301} mixture at 450 K, 0.1 MPa and $x_b = 0.5$. Results for both polymers agree well with eq 49 with $\upsilon = 0.5$, thus verifying unperturbed chain behavior. Furthermore, the linear chains exhibit a higher R_g compared to the branched chains. The ratio $g = \langle R_g^2 \rangle_b / \langle R_g^2 \rangle_l$ for this mixture is 0.729 ± 0.035. Furthermore, this ratio is equal to 0.725 ± 0.027 for the C_{121} mixture and 0.740 ± 0.018 for the C_{61} mixture. For comparison, the Zimm–Stockmayer[38–39] theory based on the random coil hypothesis predicts a value for g equal to 0.778.

An important consideration for the chain IA elementary move introduced here is whether it is able to relax the long chain molecules efficiently. Most of the elementary moves proposed in the past, including CB, CONROT, EB, DB, BPS, and BPF, were shown to be successful in this respect for the systems on which they were tested. In order to assess the new move's capability to relax long branched chains, three vectors are introduced to characterize the geometry of the triarm chains (Figure 13). These vectors are as follows: (a) The branch point vector, $\hat{\mathbf{v}}_{bp}$, that is the unit vector along the vectorial sum of the three bonds emanating from the branch point (with reference to Figure 13: $\hat{\mathbf{v}}_{bp} = (\mathbf{s}_1 + \mathbf{s}_2 + \mathbf{s}_3)/(|\mathbf{s}_1 + \mathbf{s}_2 + \mathbf{s}_3|)$), (b) the arm end-to-branch point unit vector, $\hat{\mathbf{v}}_{eb}$, and (c) the arm end-to-arm end unit vector, $\hat{\mathbf{v}}_{ee}$. An autocorrelation function is defined according to the product $\langle \hat{\mathbf{v}}_\alpha(0) \cdot \hat{\mathbf{v}}_\alpha(i) \rangle$, where $\hat{\mathbf{v}}_\alpha(0)$ and $\hat{\mathbf{v}}_\alpha(i)$ are the unit vectors of type α (here, α = bp, eb, or ee) at the beginning of the simulation and after a certain number i of MC moves.

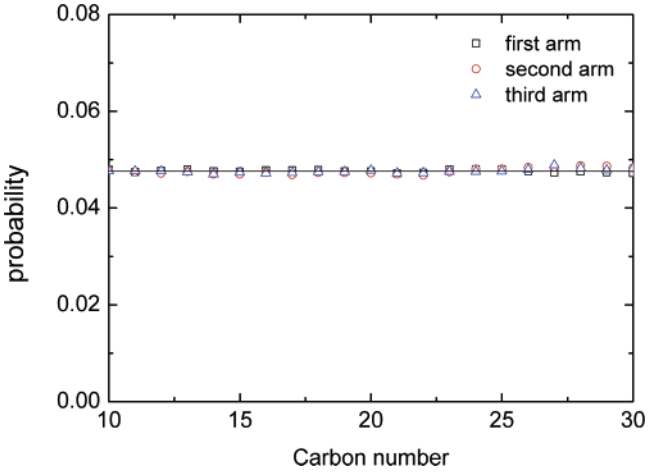

Figure 10. Probability distribution of the length (in carbon atoms) of each of the three arms of C_{61} triarm ($3 \times 20 + 1$) polyethylene in a mixture with its linear analog at 450 K, 0.1 MPa and $\beta\mu^* = 1$.

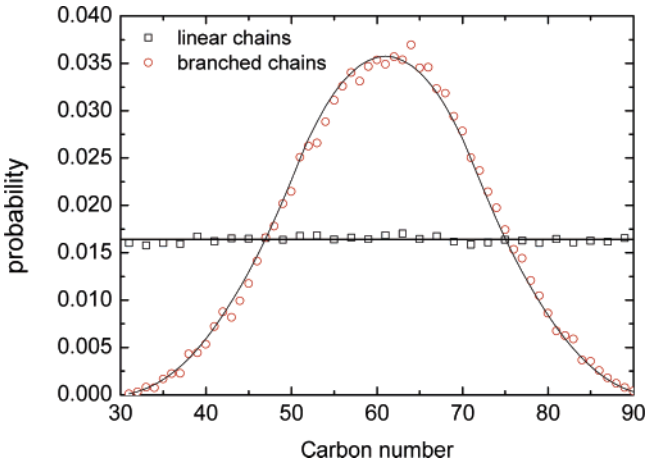

Figure 11. Probability distribution of the molecular size (in carbon atoms) of C_{61} triarm ($3 \times 20 + 1$) polyethylene and of linear C_{61} polyethylene in mixture at 450 K, 0.1 MPa and $\beta\mu^* = 1$. The solid curve is the exact mathematical expression for this distribution.[24]

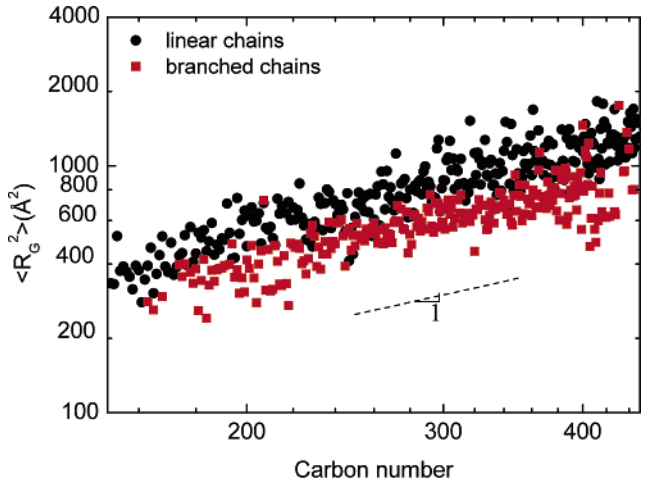

Figure 12. Double logarithmic plot of the mean squared radius of gyration, $\langle R_g^2 \rangle$, as a function of carbon number for the linear C_{301}–triarm C_{301} mixture at 450 K, 0.1 MPa and equimolar mixture. The dotted line has a slope of 1 ($\upsilon = 0.5$).

In Figure 14, the autocorrelation functions for the three characteristic unit vectors of a triarm C_{61} polyethylene in the mixture with a linear C_{61} polyethylene at 450 K, 0.1 MPa, and $\beta\mu^* = 1$ are shown. The blend of elementary MC moves used

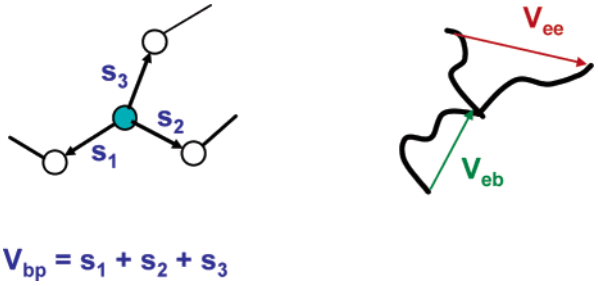

Figure 13. Schematic representation of the characteristic vectors in a triarm chain: (a) The branch point vector, $\mathbf{v}_{bp}$, is the vectorial sum of the three bond vectors emanating from the branch point, (b) the arm end-to-branch point vector, $\mathbf{v}_{eb}$, and (c) the arm end-to-arm end vector, $\mathbf{v}_{ee}$.

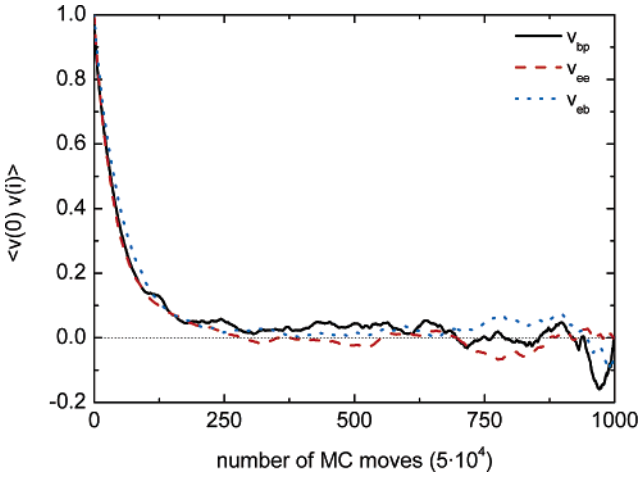

Figure 14. Relaxation of the characteristic vectors of triarm C_{61} ($3 \times 20 + 1$) polyethylene in a mixture with linear C_{61} polyethylene at 450 K, 0.1 MPa and $\beta\mu^* = 1$.

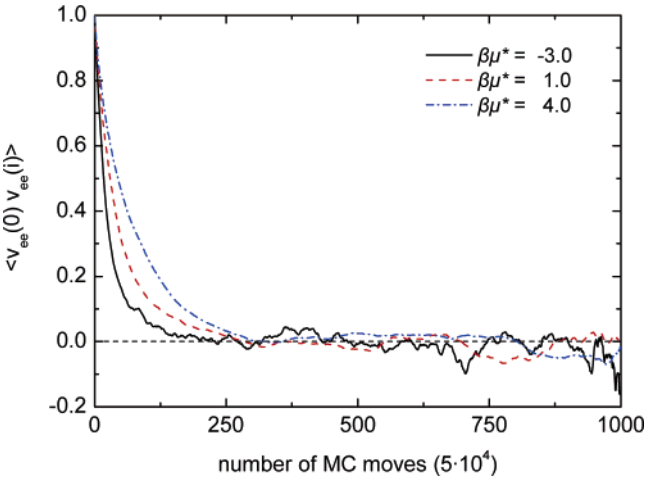

Figure 15. Relaxation of the end-to-end characteristic vector of linear C_{61} polyethylene in a mixture with triarm C_{61} ($3 \times 20 + 1$) polyethylene at 450 K, 0.1 MPa and various $\beta\mu^*$ values.

for these calculations relaxes very efficiently both the triarm chain ends as well as the branch point.

An autocorrelation function is defined also for the end-to-end unit vector of the linear chains, $\langle \hat{\mathbf{v}}_{ee}(0) \cdot \hat{\mathbf{v}}_{ee}(i) \rangle$. In Figure 15, $\langle \hat{\mathbf{v}}_{ee}(0) \cdot \hat{\mathbf{v}}_{ee}(i) \rangle$ for the linear C_{61} polyethylene in the mixture with a triarm C_{61} polyethylene at 450 K and 0.1 MPa is shown for different relative chemical potential values. In all cases, the elementary moves used relax the chains efficiently. The $\beta\mu^*$ value has a relatively small effect on the chain relaxation; the autocorrelation function decreases more slowly for larger $\beta\mu^*$

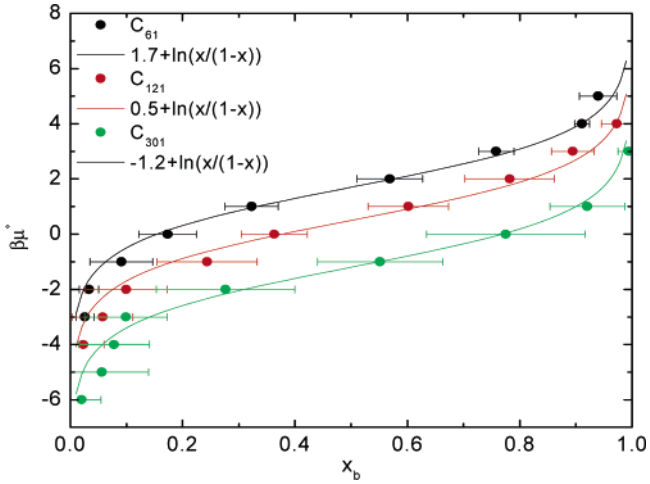

Figure 16. Relative chemical potential, $\beta\mu^*$, as a function of composition, x_b, for the mixtures: (a) linear C_{61} polyethylene−triarm C_{61} ($3 \times C_{20} + 1$) polyethylene, (b) linear C_{121} polyethylene−triarm C_{121} ($3 \times C_{40} + 1$) polyethylene, and (c) linear C_{301} polyethylene−triarm C_{301} ($3 \times C_{100} + 1$) polyethylene at 450 K and 0.1 MPa. Points are simulation results and lines are the theoretically predicted curves from eq 34. The coefficients shown in the legend are obtained by best fits to the simulation data.

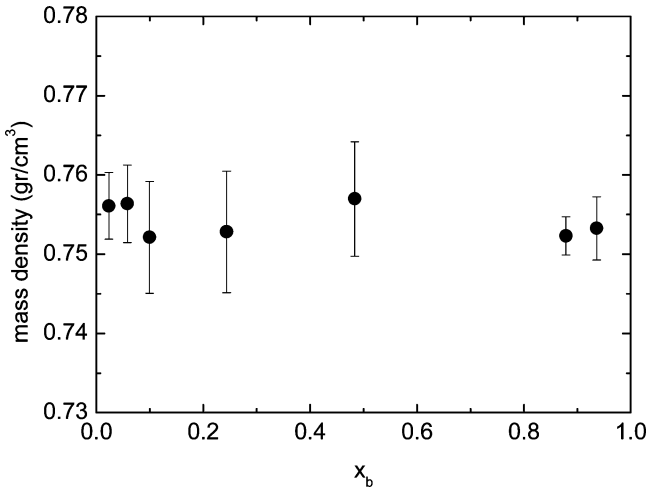

Figure 17. Mass density, ρ, as a function of composition, x_b for the mixture linear C_{121} polyethylene−triarm C_{121} ($3 \times C_{40} + 1$) polyethylene at 450 K and 0.1 MPa.

values. This should be attributed to the fact that larger $\beta\mu^*$ values correspond to lower linear chain content (x_l) and so linear chain involvement in MC moves is less frequent.

MC simulations at 450 K and 0.1 MPa and different chemical potential values were performed for the three polyolefin blends and the composition was recorded, as shown in Figure 16. In all cases, $\beta\mu^*$ varies monotonically with composition and so all three blends are fully miscible. This is an expected result, since the components in all blends are of relatively low mean molar mass (856 g/mol for the C_{61} blend, 1696 g/mol for the C_{121} blend and 4216 g/mol for the C_{301} blend) and the temperature is relatively high. At these conditions, experimental data for high-density polyethylene−low-density polyethylene blend reveal a fully miscible system.[40] Here again, as in Figure 9, theoretical calculations assuming a constant z value are in reasonably good agreement, within the statistical uncertainty, with simulation results. The mixture's close to ideal behavior can be further assessed from the mass density variation with composition. Results in Figure 17 for the case of C_{121} blend at 450 K reveal that the mass density is practically constant, within

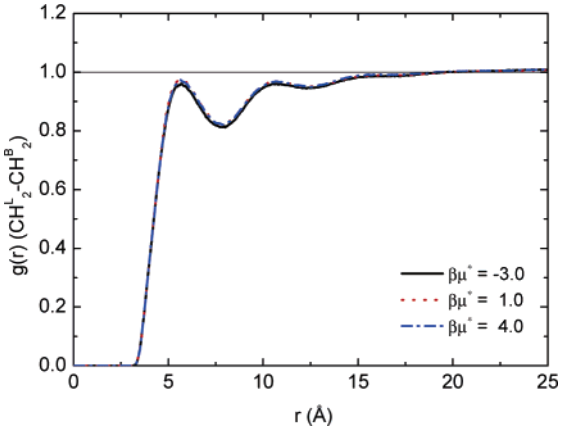

Figure 18. Radial distribution function for linear methylene-branched methylene pairs for a mixture of linear C_{61} polyethylene−triarm C_{61} ($3 \times 20 + 1$) polyethylene at 450 K, 0.1 MPa and various relative chemical potential values.

the statistical uncertainty of the simulation, over the entire composition range.

In order to evaluate the blend nonideality at the microscopic level, the radial distribution function between different UA pairs was calculated. The vast majority of UA interaction sites in both linear and triarm polyethylenes examined here are $-CH_2-$. In Figure 18, $g(r)$ for $CH_2^{(linear)} - CH_2^{(triarm)}$ pairs is shown at various chemical potential values (and, consequently, various compositions) for the C_{61} blend. Results for the different mixtures are almost indistinguishable, which indicates that correlations between segments belonging to linear and triarm chains do not change as the composition changes. In other words, one may conclude that for these systems z remains composition-independent. This is also verified by the fact that by setting the first term on the right-hand side of eq 34 constant and equal to 1.7 for the C_{61} blend, a very good description of the simulation results is obtained (Figure 16).

For considerably higher molecular weight and lower temperature values, blends are expected to deviate from ideality. Such systems require substantially higher computing power. Preliminary results for polyolefin blends at 350 K and for blends of linear and branched chains of different molecular weights reveal some deviations from ideal mixture behavior which, however, are not large enough to result in partially miscible blends. Work is still underway and will be presented in a forthcoming publication.

6. Conclusions

A new, efficient molecular simulation scheme in the framework of the semi-grand statistical ensemble was proposed for the calculation of structure, thermodynamic and phase equilibrium properties of binary linear−long branched polyolefin blends. At the same time, a new elementary MC move was developed that allows chain identity alterations (IA), from linear to branched and vice versa. In this way, the mixture composition converges to the value characteristic of the state point defined by the semi-grand ensemble and the conformations of the long chains relax efficiently. The new methodology was applied to three linear polyethylene−symmetric triarm polyethylene blends of the same mean molecular weight at 450 K and 0.1 MPa. All systems were shown to be fully miscible and to be within error bars of ideal solution thermodynamics. Future work will focus on polyolefin blends that vary greatly in molecular size, asymmetry between chain branches, temperature, and pressure.

Acknowledgment. Financial support for this work provided by the General Secretariat of Research and Technology, Greece through the PENED99 and Collaborative Research Projects with Third Countries (Project No. ΗΠΑ-010) programs to IGE is gratefully acknowledged. The CINECA Supercomputer Center in Bologna, Italy, is acknowledged for a visiting post-graduate fellowship and generous allocation of supercomputing time to LDP through the MINOS program. IGE is thankful to the Technical University of Denmark, Department of Chemical Engineering, IVC−SEP for a visiting professorship during the last part of this work, funded by the Danish Research Council for Technology and Production Sciences.

References and Notes

(1) Manson, J. A.; Sperling, L. H. *Polymer Blends and Composites*; Plenum Press: New York, 1976.
(2) Larson, R. G. *The Structure and Rheology of Complex Fluids*; Oxford University Press: New York, 1999.
(3) Bates, F. S.; Wignall, G. D.; Koehler, W. C. *Phys. Rev. Lett.* **1985**, *55*, 2425.
(4) Banaszak, M.; Petsche, I. B.; Radosz, M. *Macromolecules* **1993**, *26*, 391.
(5) Reichart, G. C.; Graessley, W. W.; Register, R. A.; Krishnamoorti, R.; Lohse, D. J. *Macromolecules* **1997**, *30*, 3363.
(6) White, J. L.; Brant, P. *Macromolecules* **1998**, *31*, 5424.
(7) White, J. L.; Lohse, D. J. *Macromolecules* **1999**, *32*, 958.
(8) Wolak, J.; Jia, X.; Gracz, H.; Stejskal, E. O.; White, J. L.; Wachowicz, M.; Jurga, S. *Macromolecules* **2003**, *36*, 4844.
(9) Jeon, H. S.; Lee, J. H.; Balsara, N. P.; Newstein, M. C. *Macromolecules* **1998**, *31*, 5340.
(10) Stephens, C. H.; Hiltner, A.; Baer, E. *Macromolecules* **2003**, *36*, 2733.
(11) Rubinstein, M.; Colby, R. H. *Polymer Physics*; Oxford University Press: New York, 2003.
(12) Puig, C. C.; Odell, J. A.; Hill, M. J.; Barham, P. J.; Folkes, M. J. *Polymer* **1994**, *35*, 2452.
(13) Schipp, C.; Hill, M. J.; Barham, P. J.; Cloke, V. M.; Higgins, J. S.; Oiarzabal, L. *Polymer* **1996**, *37*, 2291.
(14) Agamalian, M.; Alamo, R. G.; Kim, M. H.; Londono, J. D.; Mandelkern, L.; Wignall, G. D. *Macromolecules* **1999**, *32*, 3093.
(15) Vacatello, M.; Avitabile, G.; Corradini, P.; Tuzi, A. *J. Chem. Phys.* **1980**, *73*, 548.
(16) Frenkel, D.; Mooij, G. C. A. M.; Smit, B. *J. Phys.: Condens. Matter* **1992**, *4*, 3053.
(17) Siepmann, J. I.; Frenkel, D. *Mol. Phys.* **1992**, *75*, 59.
(18) de Pablo, J. J.; Laso, M.; Siepmann, J. I.; Suter, U. W. *Mol. Phys.* **1993**, *80*, 55.
(19) Dodd, L. R.; Boone, T. D.; Theodorou, D. N. *Mol. Phys.* **1993**, *78*, 961.
(20) Pant, P. V. K.; Theodorou, D. N. *Macromolecules* **1995**, *28*, 7224.
(21) Mavrantzas, V. G.; Theodorou, D. N. *Macromolecules*, **1998**, *31*, 6310.
(22) Mavrantzas, V. G.; Boone, T. D.; Zervopoulou, E.; Theodorou, D. N. *Macromolecules*, **1999**, *32*, 5072.
(23) Karayiannis, N. Ch.; Mavrantzas, V. G.; Theodorou, D. N. *Phys. Rev. Lett.* **2002**, *88*, 105503.
(24) Peristeras, L. D.; Economou, I. G.; Theodorou, D. N. *Macromolecules* **2005**, *38*, 386.
(25) Wick, C. D.; Siepmann, J. I. *Macromolecules* **2000**, *33*, 7207.
(26) Panagiotopoulos, A. Z. *Mol. Phys.* **1987**, *61*, 813.
(27) Widom, B. *Mol. Phys.* **1963**, *39*, 2808.
(28) Spyriouni, T.; Economou, I. G.; Theodorou, D. N. *Phys. Rev. Lett.* **1998**, *80*, 4466.
(29) Zervopoulou, E.; Mavrantzas, V. G.; Theodorou, D. N. *J. Chem. Phys.* **2001**, *115*, 2860.
(30) Boulougouris, G. C.; Economou, I. G.; Theodorou, D. N. *J. Chem. Phys.* **2001**, *115*, 8231.
(31) Kofke, D. A.; Glandt, E. D. *J. Chem. Phys.* **1987**, *87*, 4881.
(32) Kofke, D. A.; Glandt, E. D. *Mol. Phys.* **1988**, *64*, 1105.
(33) Modell, M.; Reid, R. C. *Thermodynamics and its Applications*; Prentice Hall: New York, 1983.
(34) Karayiannis, N. Ch.; Giannousaki, A. E.; Mavrantzas, V. G.; Theodorou, D. N. *J. Chem. Phys.* **2002**, *117*, 5465.
(35) Martin, M. G.; Siepmann, J. I. *J. Phys. Chem. B* **1998**, *102*, 2569.
(36) Martin, M. G.; Siepmann, J. I. *J. Phys. Chem. B* **1999**, *103*, 4508.
(37) de Gennes, P.-G. *Scaling Concepts in Polymer Physics;* Cornell University Press: Ithaca, NY, 1979.
(38) Zimm, B. H.; Stockmayer, W. H. *J. Chem. Phys.* **1949**, *17*, 1301.
(39) Zimm, B. H.; Kilb, R. W. *J. Polym. Sci.* **1959**, *37*, 19.
(40) Walsh, D. J.; Graessley, W. W.; Datta, S.; Lohse, D. J.; Fetters, L. J. *Macromolecules* **1992**, *25*, 5236.

MA0627121